Zhibo Wen, Patrick Henkel, Christoph Günther

Multi-Stage Satellite Phase and Code Bias Estimation

Original scientific paper

Precise point positioning with satellite navigation signals requires knowledge of satellite code and phase biases. In this paper, a new multi-stage method is proposed for estimating of these biases using measurements from a geodetic network. The method first subtracts all available a priori knowledge on orbits, satellite clocks and multipath from the measurements to reduce their dynamics. Secondly, satellite phase biases, ionospheric delays, carrier phase integer ambiguities and the geometry combining all non-dispersive parameters are jointly estimated in a Kalman filter. Finally, the a posteriori geometry estimates are refined in a second Kalman filter for the computation of orbital errors, code biases and tropospheric delays. As the first Kalman filter introduces time correlation, a generalized Kalman filter for colored measurement noise is applied in the second stage. The proposed algorithm is applied to dual frequency GPS measurements from a local geodetic network in Germany. A remarkable bias stability with variations of less than 3 cm over 4 hours is observed.

Key words: Satellite navigation, Phase biases, Code biases, Ambiguity resolution

Višerazinska procjena faznih i kodnih pomaka satelitskog signala. Precizno određivanje položaja uporabom satelitske navigacije zahtjeva poznavanje satelitskog koda te fazna mjerenja. U ovom radu predložena je nova metoda za procjenu faznih pomaka signala uporabom rezultata mjerenja iz geodetske mreže. U prvom koraku iz mjerenja se izuzimaju poznati podaci o orbitama, satelitskim satovima i višestrukim putevima, kako bi se smanjila njihova dinamika. U drugom se koraku uporabom Kalmanovog filtra procjenjuju fazni pomaci, ionosferska kašnjenja, neodređenost broja valnih duljina nosioca i geometrija koja uključuje sve nedisperzivne parametre. Konačno, određuje se korigirana geometrija u drugom Kalmanovom filtru radi proračuna orbitalnih pogrešaka, pogrešaka koda i troposferskog kašnjenja. S obzirom na to da prvi Kalmanov filtar unosi vremensku korelaciju, opći Kalmanov filtar primjenjuje se u drugom koraku. Predloženi algoritam primijenjen je u dvofrekvencijskim GPS-mjerenjima u lokalnoj geodetskoj mreži u Njemačkoj. Postignuta je visoka stabilnost rezultata uz varijacije manje od 3 cm tijekom 4 sata.

Ključne riječi: satelitska navigacija, fazni pomak, pomak koda, neodređenost rezolucije

1 INTRODUCTION

The positioning of a kinematic receiver in real-time with centimeter-level accuracy can currently only be achieved in differential mode, i.e. a relative positioning of two receivers. Double difference measurements between a pair of satellites and a pair of receivers are performed to eliminate the receiver and satellite biases and, thus, to simplify the resolution of the carrier phase ambiguities. However, this double differencing requires the exchange of the complete set of measurements, which is a major drawback and a strong motivation for precise point positioning. A prerequisite for the resolution of undifferenced integer ambiguities is the knowledge of satellite phase and code biases. Today, the International GNSS Service (IGS) [1] is providing differential P1/C1 code biases, which are computed on the basis of the ionosphere-free linear combination [2] [3].

Gabor and Nerem [4] and Laurichesse and Mercier [5] estimated the L1 and L2 phase biases by combining the fractional bias term of the Melbourne-Wübbena combination [6] and the joint bias/ ambiguity term of the geometry-preserving, ionosphere-free phase-only combination. The obtained pseudo-phase biases enable an unbiased estimation of the L1 and L2 integer ambiguities. However, these phase biases also include a weighted combination of code biases on both frequencies. It is shown in [7] that these L1/ L2 pseudo-phase biases correspond to a geometry-preserving, ionosphere-free narrowlane combination with a wavelength of only 10.7 cm.

Günther proposed a much more general measurement model, which assumes an individual phase and code bias for each satellite, receiver and frequency in [8]. As the estimation of all biases is not feasible, a Gaussian elimination

can be performed to obtain the optimal mapping of biases and ambiguities into a full-rank subspace. The proposed mapping can also be applied to triple frequency measurements, which enables the use of more attractive combinations than the currently used dual frequency Melbourne-Wübbena and ionosphere-free phase-only combinations. Zou et al. described in [9] a similar mapping, i.e. he overcame the rank defect by mapping the $R + K$ receiver and satellite biases and the $R \cdot K$ integer ambiguities into a first subset of $(R-1)(K-1)$ integer ambiguities and a second subset of $R + K - 1$ real-valued bias-ambiguity combinations. The ambiguities of the first subset correspond to the double difference ambiguities.

As the convergence of biases and ambiguities is one of the most challenging problems of precise point positioning, two cascaded Kalman filters are proposed to estimate the phase and code biases. The paper is organized as follows: Section 2 proposes the parameter mapping and consequently the full-rank measurement model; Section 3 to 5 described the subtraction of a priori knowldege and the first and second stage Kalman filter; Section 6 shows the simulation results.

2 MEASUREMENT MODEL

A very general model for the absolute carrier phase and code measurements on two frequencies is used in the approach of Günther [8]. Assuming each link bias can be treated separated $\beta_i^k = \beta_i + \beta^k$, ditto for b, i.e.

$$
\begin{aligned}
\lambda_1 \varphi_{1,i}^k(t) &= g_i^k(t) - I_{1,i}^k(t) + \lambda_1 N_{1,i}^k + \beta_{1,i} + \beta_1^k \\
&\quad + \varepsilon_{1,i}^k(t), \\
\lambda_2 \varphi_{2,i}^k(t) &= g_i^k(t) - q_{12}^2 I_{1,i}^k(t) + \lambda_2 N_{2,i}^k + \beta_{2,i} + \beta_2^k \\
&\quad + \varepsilon_{2,i}^k(t), \\
\rho_{1,i}^k(t) &= g_i^k(t) + I_{1,i}^k(t) + b_{1,i} + b_1^k + \eta_{1,i}^k(t), \\
\rho_{2,i}^k(t) &= g_i^k(t) + q_{12}^2 I_{1,i}^k(t) + b_{2,i} + b_2^k + \eta_{2,i}^k(t), \quad (1)
\end{aligned}
$$

where the indices i, k ($i \in \{1, \ldots, R\}$, $k \in \{1, \ldots, K\}$) and t represent respectively receiver, satellite and time, and $q_{12} = f_1 / f_2$ denotes the frequency ratio. The remaining parameters are explained in the following with m being the frequency index:

$\lambda_m \varphi_{m,i}^k$:	carrier phase measurement,
$\rho_{m,i}^k$:	code measurement,
g_i^k:	geometry term,
$I_{m,i}^k$:	ionospheric slant delay,
$N_{m,i}^k \in \mathbb{Z}$:	integer ambiguity,
$\beta_{m,i}$:	receiver phase bias,
β_m^k:	satellite phase bias,
$b_{m,i}$:	receiver code bias,
b_m^k:	satellite code bias,

$\varepsilon_{m,i}^k$:	phase noise and phase multipath,
$\eta_{m,i}^k$:	code noise and code multipath,

The geometry term g_i^k contains non-frequency dependent terms including the geometric range $||\vec{r}_i - \vec{r}^{,k}||$, the receiver and satellite clock offsets $c\delta_i$, $c\delta^k$, and the tropospheric slant delay T_i^k. It is described by

$$
\begin{aligned}
g_i^k(t) &= ||\vec{r}_i - \vec{r}^{,k}(t - \Delta\tau_i^k(t))|| + T_i^k(t) \\
&\quad + c\left(\delta_i(t) - \delta^k(t - \Delta\tau_i^k(t))\right), \quad (2)
\end{aligned}
$$

where the satellite clock offset refers to the time when the signal was transmitted, and thus, the signal propagation time $\Delta\tau_i^k(t)$ from the satellite to the receiver has to be considered.

Assuming the number of one type of observations on each frequency is s, one would obtain a total number of $4s$ measurements on both frequencies. However, alone the geometry terms, ionospheric slant delays, and the ambiguities would add up to $4s$ unknowns. Therefore, the system of equations (1) is rank-deficient, i.e. it is not possible to estimate all the parameters in (1). A set of parameter mappings is then applied to remove the rank-deficiency, and is explained below in steps. After each step of parameter mapping, a tilde symbol is put on top of the combined parameter.

2.1 Parameter mapping

In the first step, the receiver and satellite code biases are split into two parts according to the dependency on frequency: one part $b_{g,i}$, b_g^k to the geometry terms and the other part $b_{I,i}$, b_I^k to the ionospheric slant delays, i.e.

$$
\tilde{g}_i^k(t) = g_i^k(t) + b_{g,i} + b_g^k, \quad \tilde{I}_{1,i}^k(t) = I_{1,i}^k(t) + b_{I,i} + b_I^k, \quad (3)
$$

with

$$
\begin{aligned}
b_{g,i} &= -\frac{b_{2,i} - q_{12}^2 b_{1,i}}{q_{12}^2 - 1}, \quad b_{I,i} = \frac{b_{2,i} - b_{1,i}}{q_{12}^2 - 1}, \\
b_g^k &= -\frac{b_2^k - q_{12}^2 b_1^k}{q_{12}^2 - 1}, \quad b_I^k = \frac{b_2^k - b_1^k}{q_{12}^2 - 1}. \quad (4)
\end{aligned}
$$

The phase measurement equations are also affected since the geometry and ionospheric delay are common in code and phase measurements. The phase biases shall be adjusted to compensate for the mapped code biases, i.e.

$$
\begin{aligned}
\tilde{\beta}_{1,i} &= \beta_{1,r} - b_{g,i} + b_{I,i}, \quad \tilde{\beta}_{2,i} = \beta_{2,r} - b_{g,i} + q_{12}^2 b_{I,i}, \\
\tilde{\beta}_1^k &= \beta_1^k - b_g^k + b_I^k, \qquad \tilde{\beta}_2^k = \beta_2^k - b_g^k + q_{12}^2 b_I^k. \quad (5)
\end{aligned}
$$

In a next step, one of the satellite phase biases is absorbed in the other satellite phase biases and also mapped to the receiver phase biases, i.e.

$$
\begin{aligned}
\tilde{\tilde{\beta}}_{1,i} &= \tilde{\beta}_{1,i} + \tilde{\beta}_1^1, \quad \tilde{\tilde{\beta}}_1^k = \tilde{\beta}_1^k - \tilde{\beta}_1^1, \\
\tilde{\tilde{\beta}}_{2,i} &= \tilde{\beta}_{2,i} + \tilde{\beta}_2^1, \quad \tilde{\tilde{\beta}}_2^k = \tilde{\beta}_2^k - \tilde{\beta}_2^1, \quad (6)
\end{aligned}
$$

where as an example the phase bias from the first satellite is chosen. There exists a degree of freedom on the choice of the reference satellite.

Last but not least, a subset of ambiguities are mapped to phase biases and other ambiguities, which are projected into the following subspace according to Wen in [10]:

$$\tilde{\tilde{\beta}}_i = \tilde{\beta}_i + \sum_{N_j \in N_{\text{sub}}} c_{j,i} N_j, \quad \tilde{\tilde{\beta}}^k = \tilde{\beta}^k + \sum_{N_j \in N_{\text{sub}}} c_j^k N_j,$$

$$\tilde{N}_i^k = N_i^k + \sum_{N_j \in N_{\text{sub}}} c_{j,i}^k N_j, \tag{7}$$

where the coefficients $c_{j,i}$, c_j^k, and $c_{j,i}^k$, as well as the subset of ambiguities N_{sub} are determined by Gaussian elimination. Note that there also exists a degree of freedom on the choice of the subset.

2.2 The full-rank measurement model

After the three steps of parameter mappings, a full-rank measurement model is obtained:

$$\lambda_1 \phi_{1,i}^k(t) = \tilde{g}_i^k(t) - \tilde{I}_{1,i}^k(t) + \lambda_1 \tilde{N}_{1,i}^k + \tilde{\tilde{\beta}}_{1,i} + \tilde{\tilde{\beta}}_1^k$$
$$+ \varepsilon_{1,i}^k(t),$$

$$\lambda_2 \phi_{2,i}^k(t) = \tilde{g}_i^k(t) - q_{12}^2 \tilde{I}_{1,i}^k(t) + \lambda_2 \tilde{N}_{2,i}^k + \tilde{\tilde{\beta}}_{2,i} + \tilde{\tilde{\beta}}_2^k$$
$$+ \varepsilon_{2,i}^k(t),$$

$$\rho_{1,i}^k(t) = \tilde{g}_i^k(t) + \tilde{I}_{1,i}^k(t) + \eta_{1,i}^k(t),$$

$$\rho_{2,i}^k(t) = \tilde{g}_i^k(t) + q_{12}^2 \tilde{I}_{1,i}^k(t) + \eta_{2,i}^k(t), \tag{8}$$

which enables the estimation of the whole parameter set with a network of receivers, including the geometry terms, the ionospheric delays, the ambiguities and the phase biases.

As the code and phase measurements are in practice provided with a certain sampling rate (e.g. 1 Hz), the notation for the time index t is replaced by a discrete time index n in the following sections.

3 SUBTRACTION OF A PRIORI KNOWLEDGE

The geometry terms contain orbits of the GPS satellites, which introduces non-linearity in the state space model. Thus, it is beneficial to correct the code and phase measurements with rough range estimates, which can be calculated from the known coordinates of the reference stations and the satellite positions from the broadcast ephemeris. This enables a much stronger state space model in the Kalman filter estimation and therefore more accurate state estimates.

Moreover, if the reference stations can be observed to repeat a multipath error pattern, the bias estimation can also benefit from the correction of the multipath. To determine the multipath pattern, the observations over multiple days under same geometry conditions shall be needed.

3.1 Subtraction of range information

Since the satellite position $\hat{\vec{r}}_n^k$ and clock offset $c\delta\hat{\tau}_n^k$ are available from the broadcast ephemeris, also the receiver position $\hat{\vec{r}}_i$ available from the reference station, these a priori information shall be subtracted from the code and phase measurements, i.e.

$$\lambda_m \Delta\phi_{m,i,n}^k = \lambda_m \phi_{m,i,n}^k - ||\hat{\vec{r}}_i - \hat{\vec{r}}_n^k|| + c\delta\hat{\tau}_n^k,$$
$$\Delta\rho_{m,i,n}^k = \rho_{m,i,n}^k - ||\hat{\vec{r}}_i - \hat{\vec{r}}_n^k|| + c\delta\hat{\tau}_n^k, \tag{9}$$

which also updates the geometry term as

$$\Delta\tilde{g}_{i,n}^k = \left(\vec{e}_{i,n}^k\right)^{\mathrm{T}} \Delta\vec{r}_n^k + c\delta\tau_i + b_g^k + M_{i,n}^k T_{z,i,n}, \tag{10}$$

with $\vec{e}_{i,n}^k$ denoting the unit vector from the satellite to the receiver, M being the tropospheric mapping function and T_z representing the tropospheric zenith delay.

3.2 Multipath correction

In general, multipath estimation without constraint is not feasible in real-time processing, since multipath affects each satellite-receiver link individually and is also time-variant. However, the receiver-satellite geometry repeats every satellite revolution period (e.g. 11h 58mins 2s for GPS) for geodetic reference stations, which enables multipath estimation with measurements taken from multiple sidereal days with same satellite geometry (see Wen et al. [11]).

GPS measurements were taken from a network of geodetic SAPOS (Satellitenpositionierungsdienst der deutschen Landesvermessung) stations (see [12]) in Bavaria between May 30 and June 5 in 2011. The stations all use the same brand of receivers (in order not to introduce inter-brand receiver biases), as shown in green triangles in Fig. 1. The observation period on the last day was from 8:00 am to 9:40 am, and was shifted multiples of 3mins 56s on the other days to obtain the same satellite geometry.

A Kalman filter has been set up (detailed description in section 4) to solve the system of equations (8), where the integer nature of the ambiguities was not considered. Then, the code residuals over 7 consecutive days have been analyzed. The code residuals from station Günzburg and satellite PRN 5 are shown in Fig. 2. To illustrate the repeatability, the curves have been shifted by multiples of 2 meters to distinguish the code residuals from different days. It is obvious that the residuals experienced similar large oscillations, especially in low elevation angles.

The estimated multipath at station Günzburg is shown in Fig. 3, which is obtained from a sidereal filtering of the code residuals over a whole week. Through the sidereal
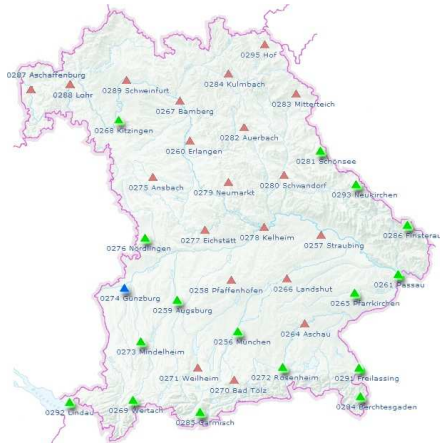
Fig. 1. *The SAPOS network in Bavaria. Green triangles indicate the stations where the observations were taken. The station Günzburg in blue triangle shows strong repeatable multipath error.*
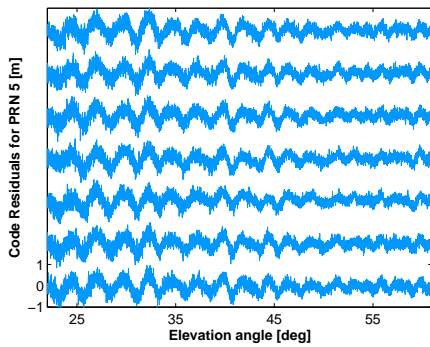

Fig. 2. *The code residuals observed at station Günzburg for PRN 5 between the observed period over a week. To distinct among others, the curves have been shifted artificially.*

Fig. 3. *The multipath estimate of the link between station Günzburg and PRN 5*

Fig. 4. *Benefit of multipath correction: The strong multipath pattern is removed, and thus the code residual contains a nearly white Gaussian noise*

filtering, the code noise on the residuals is substantially reduced. If one applies the multipath correction in the same estimation process using an independent set of measurements on June 6, most of the oscillations are removed in the code residuals and a nearly white Gaussian noise is obtained as shown in Fig. 4.

4 THE FIRST-STAGE KALMAN FILTER

Kalman filter algorithm takes advantage of the system's dynamic model and a series of measurements to estimate the time-varying states, which in most cases are more precise than those obtained by using single measurements alone [13]. A conventional Kalman filter contains a measurement model and a state space model, which are given
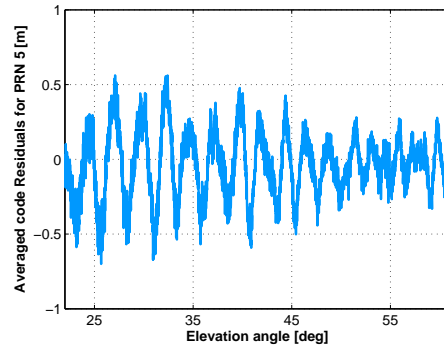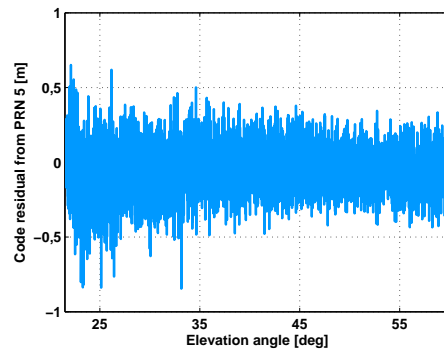
by

$$
\begin{aligned}
z_n &= H_n x_n + \zeta_n, \\
x_n &= \Phi_{n-1} x_{n-1} + w_{n-1}, \quad (11)
\end{aligned}
$$

where z_n and x_n denote respectively the measurement and state vector, H_n and Φ_n denote respectively the generation and state transition matrix, and ζ_n and w_n are measurement and process noise, which are assumed to follow white Gaussian distributions: $\zeta_n \sim \mathcal{N}(0, R_n)$, and $w_n \sim \mathcal{N}(0, Q_n)$.

At each epoch, the Kalman filter performs a prediction step of the state estimates according to the ones from the last epoch, and updates the prediction with the current measurement, i.e.

$$
\left.
\begin{aligned}
\hat{x}_n^- &= \Phi_{n-1}\hat{x}_{n-1}^+, \\
P_n^- &= \Phi_{n-1}P_{n-1}^+\Phi_{n-1}^{\mathrm{T}} + Q_{n-1},
\end{aligned}
\right\} \text{Prediction}
$$

$$
\left.
\begin{aligned}
\hat{x}_n^+ &= \hat{x}_n^- + K_n(z_n - H_n\hat{x}_n^-), \\
K_n &= P_n^- H_n^{\mathrm{T}}(H_n P_n^- H_n^{\mathrm{T}} + R_n)^{-1}, \\
P_n^+ &= (I - K_n H_n)P_n^-,
\end{aligned}
\right\} \text{Update} \quad (12)
$$

where the upper indices "-" and "+" denote a priori and a posteriori estimation respectively, and P_n is the covariance matrix of the state estimate.

A first-stage Kalman filter is implemented to estimate the geometry, the ionospheric slant delay, the ambiguities and the phase biases in equation (8). The geometry is treated as a whole parameter and not yet split into position domain, which helps the convergence and fixings of the ambiguities and thereby the stability of the biases. The state vector reads

$$
\begin{aligned}
x = \Big(& \Delta\tilde{g}_1^1, \ldots, \Delta\tilde{g}_1^{K_1}, \ldots, \Delta\tilde{g}_R^{K_R}, \Delta\dot{\tilde{g}}_1^1, \ldots, \Delta\dot{\tilde{g}}_R^{K_R}, \\
& \tilde{I}_1^1, \ldots, \tilde{I}_R^{K_R}, \dot{\tilde{I}}_1^1, \ldots, \dot{\tilde{I}}_R^{K_R}, \tilde{\bar{\beta}}_1, \ldots, \tilde{\bar{\beta}}_R, \tilde{\bar{\beta}}^2, \ldots, \tilde{\bar{\beta}}^K, \\
& \tilde{N}_1^1, \ldots, \tilde{N}_R^{K_R} \Big)^{\mathrm{T}},
\end{aligned}
\tag{13}
$$

with each item being a vector containing all the representing parameters.

The state covariance matrix for geometry and geometry-rate or ionospheric delay and its drift was derived by Brown et al. in [13] and reads

$$
Q = S_{\mathrm{p}} \cdot \begin{pmatrix} \Delta t^4/4 & \Delta t^3/2 \\ \Delta t^3/2 & \Delta t^2 \end{pmatrix} \otimes \mathbf{1}^{s \times s},
\tag{14}
$$

with S_{p} denoting the spectral amplitude, Δt being the epoch interval, and $\otimes$ representing the Kronecker product. The amplitude in the process noise has been set to 10 cm for the range rate, and 1 cm for the ionospheric drift. No process noise is assumed for the ambiguities and the phase biases in this paper.

4.1 Sequential ambiguity fixing

The integer nature of the ambiguities shall be exploited to further improve the stability of the bias estimates. The ambiguities are fixed sequentially during the first-stage Kalman filter, where a subset is fixed to integers if the float ones have converged to an integer value over a time window, i.e.

$$
\sum_{i=1}^{T_{\mathrm{p}}} f(\hat{N}_{m,r,n-i}^{+,k}) \geq T_{\mathrm{p}} \cdot p,
\tag{15}
$$

where T_{p} denotes the time window, p represents a probability that allows some outliers, and the indicator function f reads

$$
f(\hat{N}_{m,r,i}^{+,k}) = \begin{cases} 1 & \text{if } \left| \hat{N}_{m,r,i}^{+,k} - [\hat{N}_{m,r,i}^{+,k}] \right| < e_{\mathrm{th}} \\ 0 & \text{else} \end{cases},
\tag{16}
$$

with e_{th} being the threshold. In the implementation, the parameters have been chosen as $T_{\mathrm{p}} = 600$ epochs, $e_{\mathrm{th}} = 0.08$ cycles, and $p = 95\%$.

4.2 Change of satellite visibility

The described algorithm can also be applied to estimate the biases in a long period of time, and thus, one has to take into account the change of satellite visibility, as described by Wen et al. in [14].

This includes two scenarios: A setting satellite removes the satellite-receiver links, as well as the associated ambiguities. However, the already mapped ambiguities in equation (7) shall be continuously tracked. The satellite phase bias shall be also removed from the state vector, if that satellite is no longer visible to all the stations in the network. It can be re-initialized with the converged value when the satellite rises up again.

Another scenario is the rising case, where new states are introduced to the system and new parameter mappings are performed. If a satellite is only rising at some stations and was already visible at other stations, the phase bias estimate from that satellite would benefit from increasing number of measurements. Otherwise, the states including the range, ionospheric delay, phase bias as well as the ambiguities shall be initialized and added into the system.

5 THE SECOND-STAGE KALMAN FILTER

5.1 Colored measurement noise

In the second-stage Kalman filter, according to equation (10) the geometry term is split into orbit corrections, receiver code bias/clock offset, satellite code bias and tropospheric zenith delay, which are included in the state vector given by

$$
\begin{aligned}
y_n = \Big(& \Delta\vec{r}_n^{1,\mathrm{T}}, \ldots, \Delta\vec{r}_n^{K,\mathrm{T}}, \Delta\dot{\vec{r}}_n^{1,\mathrm{T}}, \ldots, \Delta\dot{\vec{r}}_n^{K,\mathrm{T}}, c\delta\tau_1, \ldots, \\
& c\delta\tau_R, b_g^2, \ldots, b_g^K, T_{\mathrm{z},1,n}, \ldots, T_{\mathrm{z},R,n} \Big)^{\mathrm{T}}.
\end{aligned}
\tag{17}
$$

A linear state space model is assumed for the orbit correction, i.e.

$$
\begin{aligned}
\Delta\vec{r}_n^k &= \Delta\vec{r}_{n-1}^k + \Delta t \Delta\dot{\vec{r}}_{n-1}^k + w_{\Delta\vec{r}_{n-1}^k}, \\
\Delta\dot{\vec{r}}_n^k &= \Delta\dot{\vec{r}}_n^k + w_{\Delta\dot{\vec{r}}_n^k},
\end{aligned}
\tag{18}
$$

where the first order derivative of the orbit corrections is assumed to follow a random walk process.

The a posteriori geometry estimate $\Delta\hat{\tilde{g}}_n^+$ from the first-stage Kalman filter is taken as the measurement for the second-stage Kalman filter. The measurement noise ϑ_n is then the estimation error in $\Delta\hat{\tilde{g}}_n^+$, i.e.

$$
\vartheta_n = \Delta\hat{\tilde{g}}_n^+ - \Delta\tilde{g}_n.
\tag{19}
$$

According to the prediction and update equations in (12), the estimation error in the first Kalman filter is cal-

culated as

$$
\begin{aligned}
\hat{x}_n^+ - x_n &= \hat{x}_n^- + K_n \cdot (z_n - H_n \hat{x}_n^-) - x_n \\
&= \Phi_{n-1}\hat{x}_{n-1}^+ + K_n \cdot (z_n - H_n \Phi_{n-1}\hat{x}_{n-1}^+) - x_n \\
&= (I - K_n H_n)\Phi_{n-1}\hat{x}_{n-1}^+ + K_n(H_n x_n + v_n) - x_n \\
&= (I - K_n H_n)\Phi_{n-1}\hat{x}_{n-1}^+ - \\
&\quad (I - K_n H_n)(\Phi_{n-1}x_{n-1} + w_{n-1}) + K_n v_n \\
&= (I - K_n H_n)\Phi_{n-1}(\hat{x}_{n-1}^+ - x_{n-1}) + \\
&\quad (I - K_n H_n)w_{n-1} + K_n v_n,
\end{aligned} \tag{20}
$$

which shows that there exists a cross-correlation between a posteriori state estimates over consecutive epochs, i.e.

$$
\begin{aligned}
E&\left\{ \left(\hat{x}_n^+ - E\{\hat{x}_n^+\}\right) \left(\hat{x}_{n-1}^+ - E\{\hat{x}_{n-1}^+\}\right)^{\mathrm{T}} \right\} \\
&= (I - K_n H_n)\Phi_{n-1}P_{n-1}^+.
\end{aligned} \tag{21}
$$

Therefore, equation (19) is further derived as

$$
\begin{aligned}
E\left\{\vartheta_n \vartheta_{n-1}^{\mathrm{T}}\right\} &= (I - K_{n,g}H_{n,g})\Phi_{n-1,g} \cdot \\
&\quad E\left\{ \left(\Delta\hat{\tilde{g}}_{n-1}^+ - \Delta\tilde{g}_{n-1}\right) \left(\Delta\hat{\tilde{g}}_{n-1}^+ - \Delta\tilde{g}_{n-1}\right)^{\mathrm{T}} \right\} \\
&= (I - K_{n,g}H_{n,g})\Phi_{n-1,g}P_{n-1,g}^+,
\end{aligned} \tag{22}
$$

where the lower index g in the matrix notations denotes the corresponding geometry sub-matrices.

Hence, the measurement noise in the second-stage Kalman filter is colored, which harms the white Gaussian noise assumptions of a conventional Kalman filter. Bryson and Henrikson proposed a generalized Kalman filter with colored measurement noise in [15], where matrix Γ_n is introduced to describe the linear dependency of the measurement noise between consecutive epochs, i.e.

$$
\vartheta_n = \Gamma_{n-1}\vartheta_{n-1} + \zeta_{n-1}, \tag{23}
$$

with $\zeta_n \sim \mathcal{N}(0, R_n)$. As a result, one also obtains the temporal correlation as

$$
\begin{aligned}
E\{\vartheta_n \vartheta_{n-1}^{\mathrm{T}}\} &= \Gamma_{n-1} \cdot E\{\vartheta_{n-1}\vartheta_{n-1}^{\mathrm{T}}\} \\
&= \Gamma_{n-1} \cdot P_{n-1}^+.
\end{aligned} \tag{24}
$$

Combining equation (22) and equation (24) yields

$$
\Gamma_{n-1} = (I - K_n H_n)\Phi_{n-1}. \tag{25}
$$

5.2 Method of Bryson and Henrikson to decorrelate the output of the first-stage Kalman filter

Bryson and Henrikson suggested an approach in [15] to whiten the measurement noise by introducing a transformed measurement vector, denoted with an upper $*$ in the following equation

$$
z_n^* = z_{n+1} - \Gamma_n z_n, \tag{26}
$$

where $z_n = \Delta\hat{\tilde{g}}_n^+$. To clarify the notations with Eq. (11), in the following the measurement vector z_n, the generate matrix H_n, the state transition matrix Φ_n, the process noise w_n, the measurement and the process noise covariance matrices R_n and Q_n all refer to the second stage.

Applying the equations in (11) yields

$$
\begin{aligned}
z_n^* &= H_{n+1}y_{n+1} + \vartheta_{n+1} - \Gamma_n \left(H_n y_n + \vartheta_n\right) \\
&= H_{n+1}\left(\Phi_n \vartheta_n + w_n\right) + \Gamma_n \vartheta_n + \zeta_n \\
&\quad - \Gamma_n \left(H_n y_n + \vartheta_n\right) \\
&= \left(H_{n+1}\Phi_n - \Gamma_n H_n\right)y_n + H_{n+1}w_n + \zeta_n \\
&= H_n^* y_n + \vartheta_n^*,
\end{aligned} \tag{27}
$$

with the transformed generation matrix and transformed measurement noise being defined as

$$
\begin{aligned}
H_n^* &\triangleq H_{n+1}\Phi_n - \Gamma_n H_n \\
\vartheta_n^* &\triangleq H_{n+1}w_n + \zeta_n.
\end{aligned} \tag{28}
$$

The "new" measurement noise is whitened, since both w_n and ζ_n are assumed white Gaussian. However, a correlation between measurement noise ϑ_n^* and process noise w_n is introduced, i.e.

$$
\begin{aligned}
E\{w_n \vartheta_m^{*\mathrm{T}}\} &= E\{w_n \left(H_{m+1}w_m + \zeta_m\right)^{\mathrm{T}}\} \\
&= \left(Q_n H_{n+1}^{\mathrm{T}}\right)\delta_{nm} \\
&\triangleq S_n \delta_{nm},
\end{aligned} \tag{29}
$$

with δ_{nm} being the kronecker delta function. To decouple the noise, a transformed process noise is also needed. Adding a zero term in the state space model in equation (11) gives

$$
\begin{aligned}
y_n &= \Phi_{n-1}y_{n-1} + w_{n-1} \\
&\quad + J_{n-1}\left(z_{n-1}^* - H_{n-1}^* y_{n-1} - \vartheta_{n-1}^*\right), \\
&= \Phi_{n-1}^* y_{n-1} + w_{n-1}^* + J_{n-1}z_{n-1}^*,
\end{aligned} \tag{30}
$$

where the transformed state transition matrix and process noise are defined as

$$
\begin{aligned}
\Phi_n^* &\triangleq \Phi_n - J_n H_n^*, \\
w_n^* &\triangleq w_n - J_n \vartheta_n^*,
\end{aligned} \tag{31}
$$

and matrix J_n shall be chosen such that the "new" process noise is uncorrelated with the "new" measurement noise, i.e.

$$
\begin{aligned}
E\{w_n^* \vartheta_m^{*\mathrm{T}}\} &= E\{\left(w_n - J_n \vartheta_n^*\right)\vartheta_m^{*\mathrm{T}}\} \\
&= \left(S_n - J_n R_n^*\right)\delta_{nm} \overset{!}{=} 0,
\end{aligned} \tag{32}
$$

which solves for J_n as

$$
J_n = S_n (R_n^*)^{-1}. \tag{33}
$$

(a) No multipath correction

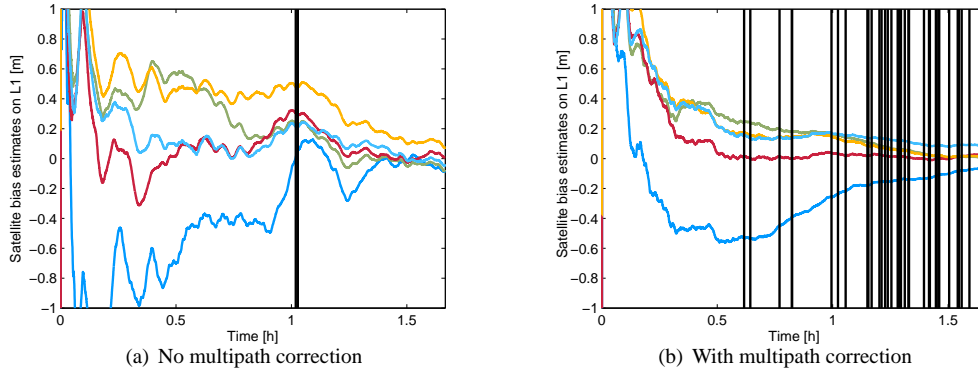(b) With multipath correction

Fig. 5. Satellite bias estimation without and with multipath correction. The multipath error propagates into the phase bias estimates which show large variations over time. The corrections remove the oscillations on the phase bias estimates and thus enable more stable bias estimates. The integer ambiguity fixing benefits from the corrections, where a much earlier fixing and much more fixings (40 out of 90 instead of 2) are enabled.

The transformed measurement and process noise are white Gaussian, and no longer correlated. Consequently, the prediction and update steps of the generalized Kalman filter, which shall be used in the second-stage, are given by (see Wang et al. [16], Wen et al. [11])

$$\left.\begin{array}{l} \hat{y}_n^- = \Phi_{n-1}^* \hat{y}_{n-1}^+ + J_{n-1} z_{n-1}^*, \\ P_n^- = \Phi_{n-1}^* P_{n-1}^+ \Phi_{n-1}^{*\mathrm{T}} + Q_{n-1}^*, \end{array}\right\} \text{Prediction}$$

$$\left.\begin{array}{l} \hat{y}_n^+ = \hat{y}_n^- + K_n \left(z_n^* - H_n^* \hat{y}_n^- \right), \\ K_n = P_n^- H_n^{*\mathrm{T}} \left(H_n^* P_n^- H_n^{*\mathrm{T}} + R_n^* \right)^{-1}, \\ P_n^+ = \left(I - K_n H_n^* \right) P_n^-, \end{array}\right\} \text{Update}$$

$$(34)$$

where the covariance matrix for the transformed process noise Q_n^* and the covariance matrix for the transformed measurement noise R_n^* are calculated respectively as

$$\begin{aligned} Q_n^* &= E\{w_n^* w_n^{*\mathrm{T}}\} \\ &= E\{(w_n - J_n \vartheta_n^*)(w_n - J_n \vartheta_n^*)^{\mathrm{T}}\} \\ &= E\{(w_n - S_n (R_n^*)^{-1} \vartheta_n^*)(w_n - S_n (R_n^*)^{-1} \vartheta_n^*)^{\mathrm{T}}\} \\ &= Q_n - S_n (R_n^*)^{-1} S_n^{\mathrm{T}} - S_n ((R_n^*)^{-1})^{\mathrm{T}} S_n^{\mathrm{T}} + \\ &\quad S_n (R_n^*)^{-1} R_n^* ((R_n^*)^{-1})^{\mathrm{T}} S_n^{\mathrm{T}} \\ &= Q_n - S_n (R_n^*)^{-1} S_n^{\mathrm{T}}, \end{aligned} \qquad (35)$$

and

$$\begin{aligned} R_n^* &= E\{\vartheta_n^* \vartheta_n^{*\mathrm{T}}\} \\ &= E\{(H_{n+1} w_n + \zeta_n)(H_{n+1} w_n + \zeta_n)^{\mathrm{T}}\} \\ &= H_{n+1} Q_n H_{n+1}^{\mathrm{T}} + R_n. \end{aligned} \qquad (36)$$

The noise covariance matrix R_n in equation (36) can be obtained by applying equation (23), (24), (25) as

$$\begin{aligned} R_n &= E\{\zeta_n \zeta_n^{\mathrm{T}}\} \\ &= E\{(\vartheta_{n+1} - \Gamma_n \vartheta_n)(\vartheta_{n+1} - \Gamma_n \vartheta_n)^{\mathrm{T}}\} \\ &= E\{\vartheta_{n+1} \vartheta_{n+1}^{\mathrm{T}}\} - \Gamma_n E\{\vartheta_n \vartheta_{n+1}^{\mathrm{T}}\} - E\{\vartheta_{n+1} \vartheta_n^{\mathrm{T}}\} \Gamma_n^{\mathrm{T}} \\ &\quad + \Gamma_n E\{\vartheta_n \vartheta_n^{\mathrm{T}}\} \Gamma_n^{\mathrm{T}} \\ &= E\{\vartheta_{n+1} \vartheta_{n+1}^{\mathrm{T}}\} - \Gamma_n E\{\vartheta_n \vartheta_n^{\mathrm{T}}\} \Gamma_n^{\mathrm{T}} - \Gamma_n E\{\vartheta_n \vartheta_n^{\mathrm{T}}\} \Gamma_n^{\mathrm{T}} \\ &\quad + \Gamma_n E\{\vartheta_n \vartheta_n^{\mathrm{T}}\} \Gamma_n^{\mathrm{T}} \\ &= E\{\vartheta_{n+1} \vartheta_{n+1}^{\mathrm{T}}\} - \Gamma_n E\{\vartheta_n \vartheta_n^{\mathrm{T}}\} \Gamma_n^{\mathrm{T}} \\ &= P_{n+1}^+ - \Gamma_n P_n^+ \Gamma_n^{\mathrm{T}}. \end{aligned} \qquad (37)$$

6 RESULTS

In this section, some results from real GPS measurements as well as from simulations are shown, where the results from the first-stage Kalman filter are shown in subsection 6.1, and the ones from the second-stage are shown in subsection 6.2.

6.1 Results from the first-stage Kalman filter

The same network of stations has been chosen as in subsection 3.2, and the measurements of May 30, 2011 have been processed. Fig. 5 shows the satellite phase bias estimates without and with the multipath correction, where the ambiguities are fixed sequentially. Each black vertical line indicates a fixing of one float ambiguity. The bias estimates are much more smoothed in Fig.5(b), since the large oscillations caused by multipath errors are removed. This involves that the first fixing of ambiguities happened almost within half the time and 38 additional ambiguities are fixed. The stability of the bias estimates is improved accordingly.

Long term phase bias estimation is also realized with GPS measurements processed 24 hours on March 14, 2011, where 11 stations from the SAPOS network in Fig. 1 was selected. The method described in subsection 4.2 was applied. The phase bias estimates from PRN 10 and 24 on both frequencies are shown in figures 6 and 7. The temporal variations of the converged bias estimates reach around 3 cm, and show a high correlation between both frequencies.
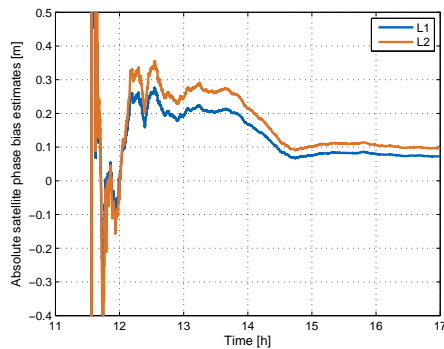

Fig. 6. Absolute satellite phase bias estimates of PRN 10 on both frequencies, which was estimated the total visible period
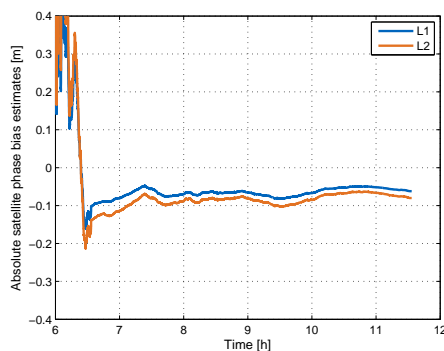

Fig. 7. Absolute satellite phase bias estimates of PRN 24 on both frequencies, which has shown a high stability over the total visible period

6.2   Results from the second-stage Kalman filter

A simulation has been performed in this subsection. The Galileo code and phase measurements were generated with a network of 39 IGS worldwide stations, based on generated orbit corrections, receiver clock offsets, satellite code biases, ionospheric delays, receiver and satellite code biases, integer ambiguities. The tropospheric delay is assumed to be perfectly known and corrected. The

dual-stage Kalman filter algorithm is applied, where in the second-stage the in-, and cross-track orbit corrections are estimated for all visible satellites.

Fig 8 shows the difference between the generated and estimated orbit corrections (for space reason only shown for satellite PRN 2 to 5), where the converged error were under 2 cm for most of the time. Fig 9 shows the errors in the satellite code bias estimates for the same four PRNs, which have reached the level of 1 cm after 300 epochs.
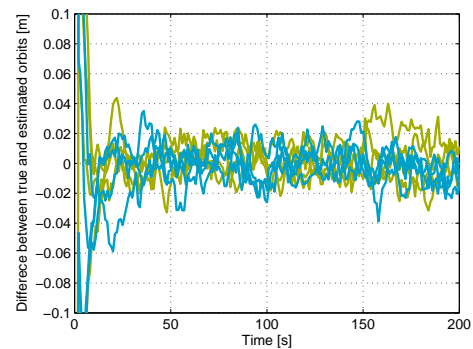

Fig. 8. The estimation error of orbit corrections, i.e. light green curves indicate the in-track errors, and blue curves the cross-track errors
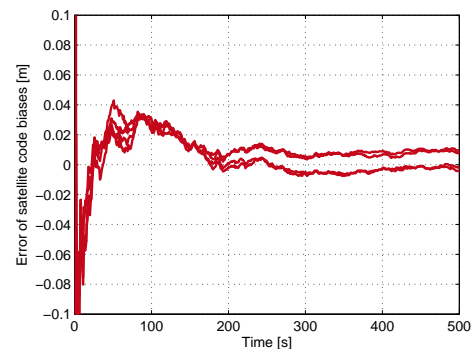

Fig. 9. The estimation error of satellite code biases

7   CONCLUSION

In this work, a dual-stage Kalman filter has been proposed for the estimation of the satellite code and phase biases with a network of stations using dual frequency GPS measurements. A sidereal filtering has been applied to estimate the code multipath, which resulted in an almost complete mitigation of the multipath on real data and in a significant high number of ambiguity fixings. The estimation was performed in two steps, where the temporal correlation in the state estimates introduced by the first-stage

Kalman filter was removed with the method of Bryson and Henrikson. Simulation results show that the error in orbit corrections and satellite code biases converge under 2 cm.

REFERENCES

[1] "International GNSS Services" Online: http://igscb.jpl.nasa.gov/, accessed on: on Mar. 20, 2012.

[2] R. Dach, U. Hugentobler, P. Fridez and M. Meindl, *Bernese GPS Software*, Jan. 2007

[3] S. Schaer and P. Steigenberger, "Determination and use of GPS differential code bias values", *IGS Workshop*, Darmstadt, Germany, May 2006.

[4] M. Gabor and S. Nerem, "Satellite-satellite single difference phase calibration as applied to ambiguity resolution", *Navigation*, vol. 49, no. 4, pp. 223-247, 2002.

[5] D. Laurichesse and F. Mercier, Integer ambiguity resolution on undifferenced GPS phase measurements and its application to PPP, *Proc. of ION-GNSS*, Forth Worth, USA, pp. 135-149, Sep. 2007.

[6] G. Wübbena, GPS carrier phases and clock modeling, *Lecture Notes in Earth Sciences: GPS-Techniques Applied to Geodesy and Surveying*, vol. 19, pp. 381-392, 1988.

[7] P. Henkel, Z. Wen and C. Günther, "Estimation of satellite and receiver biases on multiple Galileo frequencies with a Kalman filter", *Proc. of ION Intern. Techn. Meet.*, pp. 1067-1074, San Diego, USA, Jan. 2010.

[8] C. Günther, Satellite Navigation, *Lecture Note*, to be published, Technische Universität München, 2010.

[9] X. Zou, W.-M. Tang, M. Ge, J. Liu and H. Cai, "A New Network RTK based on Transparent Reference Selection in Absolute Positioning Mode", *J. of Surveying Engineering*, submitted, 2012.

[10] Z. Wen, "Estimation of Code and Phase Biases in Satellite Navigation", *Master thesis*, Technische Universität München, 2010.

[11] Z. Wen, P. Henkel, M. Davaine and C. Günther, "Satellite phase and code bias estimation with cascaded Kalman filter", *Proc. of Europ. Nav. Conf.*, London, UK, Oct. 2011.

[12] SAPOS Bayern - Referenzstationen, Bayerische Vermessungsverwaltung, *http://sapos.bayern.de*, accessed on Jun. 7, 2011.

[13] R. Brown and P. Hwang, *Introduction to random signals and applied Kalman filtering*, 3rd edition, John Wiley & Sons, New York, 1997.

[14] Z. Wen, P. Henkel, and C. Günther, "Reliable estimation of phase biases of GPS satellites with a local reference network", *Proc. of 53rd IEEE Intern. Symposium ELMAR*, Zadar, Croatia, pp. 321-324, Sept. 2011.

[15] A. E. Bryson, Jr. and L. J. Henrikson, "Estimation using sampled-data containing sequentially correlated noise", *J. of Spacecraft and Rockets*, 5(6), 662-665, 1968.

[16] K. Wang, Y. Li, and C. Rizos, "The practical approach to Kalman filtering with time-correlated measurement errors", *IEEE Trans. on Aero. & Electr. Sys.*, 2010.

Zhibo Wen is currently a PhD candidate at the Institute for Communications and Navigation, Technische Universität München, working on precise point positioning. He received his bachelor degree in electrical engineering from Shanghai Jiao Tong University in China, and his master degree in electrical engineering and information technology from Technische Universität München, Germany, with the rating passed high distinction in 2010. During his master studies, he has received a DAAD scholarship and an MAN scholarship for his excellent grades. He has received the "Leo-Brandt-Preis - DGON Master of Navigation" from the German Institute of Navigation for his master thesis on estimation of code and phase bias in satellite navigation.

Patrick Henkel studied electrical engineering and information technology at the Technische Universität München, Munich, Germany, and the École Polytechnique de Montréal, Canada. He then started his PhD on reliable carrier phase positioning and graduated in 2010 with "summa cum laude". He is now working towards his habilitation in the field of precise point positioning. He was a guest researcher at TU Delft in 2007, and at the GPS Lab at Stanford University, Stanford, in 2008 and 2010. Patrick received the Pierre Contensou Gold Medal at the Intern. Astronautical Congress in 2007, the Bavarian regional prize at the European Satellite Navigation Competition in 2010, and the "Vodafone Förderpreis" for his dissertation in 2011. He is also one of the founders of Advanced Navigation Solutions - ANAVS GmbH.

Christoph Günther studied theoretical physics at the Swiss Federal Institute of Technology in Zurich. He received his diploma in 1979 and completed his PhD in 1984. He worked on communication and information theory at Brown Boveri and Ascom Tech. From 1995, he led the development of mobile phones for GSM and later dual mode GSM/Satellite phones at Ascom. In 1999, he became head of the research department of Ericsson in Nuremberg. Since 2003, he is the director of the Institute of Communication and Navigation at the German Aerospace Center (DLR) and since December 2004, he additionally holds a Chair at the Technische Universität München (TUM). His research interests are in satellite navigation, communication and signal processing.

AUTHORS' ADDRESSES

Zhibo Wen, M.Sc.
Patrick Henkel, Ph.D.
Prof. Christoph Günther, Ph.D.
Institute for Communications and Navigation,
Faculty of Electrical Engineering and Information Technology,
Technische Universität München,
Theresienstrasse 90, DE-80333, Munich, Germany
email: zhibo.wen@tum.de,patrick.henkel@tum.de,
christoph.guenther@tum.de